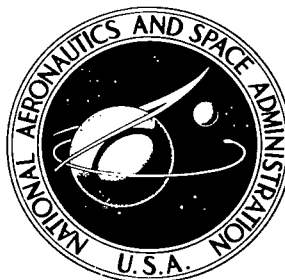


NASA TECHNICAL NOTE



NASA TN D-4882

C.1

NASA TN D-4882



LOAN COPY: RETURN TO
AFWL (WLIL-2)
KIRTLAND AFB, N MEX

EFFECT OF TURBULENT MIXING ON
AVERAGE FUEL TEMPERATURES IN
A GAS-CORE NUCLEAR ROCKET ENGINE

by Albert F. Kascak and Annie J. Easley

*Lewis Research Center
Cleveland, Ohio*

NATIONAL AERONAUTICS AND SPACE ADMINISTRATION • WASHINGTON, D. C. • NOVEMBER 1968

NASA TN D-4882

TECH LIBRARY KAFB, NM



0131509

**EFFECT OF TURBULENT MIXING ON AVERAGE FUEL TEMPERATURES
IN A GAS-CORE NUCLEAR ROCKET ENGINE**

By Albert F. Kascak and Annie J. Easley

Lewis Research Center
Cleveland, Ohio

NATIONAL AERONAUTICS AND SPACE ADMINISTRATION

For sale by the Clearinghouse for Federal Scientific and Technical Information
Springfield, Virginia 22151 - CFSTI price \$3.00

ABSTRACT

A heat-transfer analysis was made for a coaxial-flow nuclear rocket. The analysis considers one-dimensional radial transfer of heat, by both radiation and turbulent mixing from a centrally located fissioning gas to a coaxially flowing propellant. The results compare the effective thermal conductivities for radiation and turbulent mixing. Also included are typical radial-temperature profiles at various axial locations and average fuel temperatures showing the effect of neglecting turbulent mixing. Turbulent mixing had a large effect on local temperature in regions where the fuel density was smallest. Therefore, the effect of turbulent mixing on the average fuel temperature was small.

EFFECT OF TURBULENT MIXING ON AVERAGE FUEL TEMPERATURES

IN A GAS-CORE NUCLEAR ROCKET ENGINE

by Albert F. Kascak and Annie J. Easley

Lewis Research Center

SUMMARY

Heat transfer in a coaxial-flow, gas-fueled nuclear rocket with a specific impulse of 1500 seconds and a thrust between 0.445 and 4.45 meganewtons (0.1 and 1.0 Mlb) was analyzed. In this type of rocket, a low-velocity, fissioning, gaseous fuel is injected so as to flow axially down the center of a cylindrical reactor cavity. A high-velocity, hydrogen propellant flows coaxially around the fuel. Heat is generated by the fissioning fuel and is transported to the propellant. Past analyses have assumed radiation to be the principal mechanism of heat transfer. Other analyses have shown turbulent mixing to be the dominant means of mass transfer. The object of this study was to determine the effect of turbulent mixing on the transport of heat.

The present analysis considers one-dimensional radial transfer of heat by both radiation and turbulent mixing. Effective thermal conductivities for radiation and for turbulent mixing are used. The effective radiation conductivity is based on the Rosseland diffusion formulation of radiative transport, and the turbulent conductivity is based on an empirical eddy viscosity model.

The results of this study include the following:

1. Eddy viscosities obtained by scaling isothermal fluid dynamic results
2. Comparison of the effective conductivities for radiation and turbulent mixing
3. Typical radial-temperature profiles at selected axial locations
4. Average fuel temperatures showing the effect of turbulent mixing

These results showed that the change in the average fuel temperature was less than 1 percent when the heat transferred by the turbulent mixing was included. Turbulent mixing had a large effect on temperatures in regions where the fuel density was smallest. This conclusion is valid unless eddy viscosities have been underestimated by at least several orders of magnitude. Although these conclusions were drawn for a particular reactor geometry and flow distribution, changes in these factors would not cause order-of-magnitude changes in the eddy viscosities.

INTRODUCTION

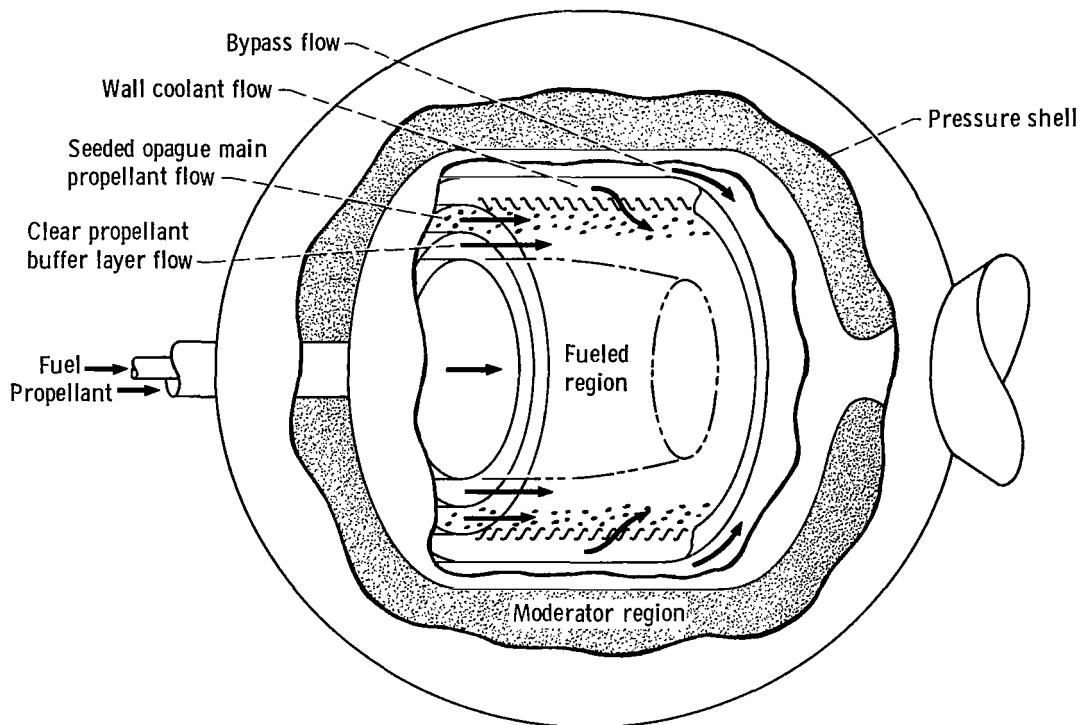
The gas-fueled nuclear rocket is a proposed propulsion concept that has high specific impulse and relatively high thrust. One configuration, illustrated in figure 1(a), is known as the coaxial-flow, gas-fueled nuclear rocket. In this concept, a low-velocity, fissioning gas fuel flows along the axis of a cylindrical cavity. The propellant flows coaxially at high velocity around the central fuel region. The objectives of using this concept are to transfer energy from the hot fuel to the colder propellant and to minimize erosion of the fuel by the propellant.

To minimize fuel-propellant mixing, an intermediate-velocity buffer layer is placed adjacent to the fuel. The buffer layer may be either hydrogen or some other gas whose molecular weight is between that of the fuel and the propellant. The propellant to be heated is seeded with opaque solid particles to increase its opacity; it flows between the fuel-buffer layer and the porous wall. Unseeded propellant provides transpiration cooling of the porous wall. Reference 1 recommends bypassing part of the propellant to increase the fueled region and to reduce the seeded propellant velocity and thereby reduce fuel-propellant mixing. Due to mixing, these flow regions are not distinguishable at all points in the reactor cavity.

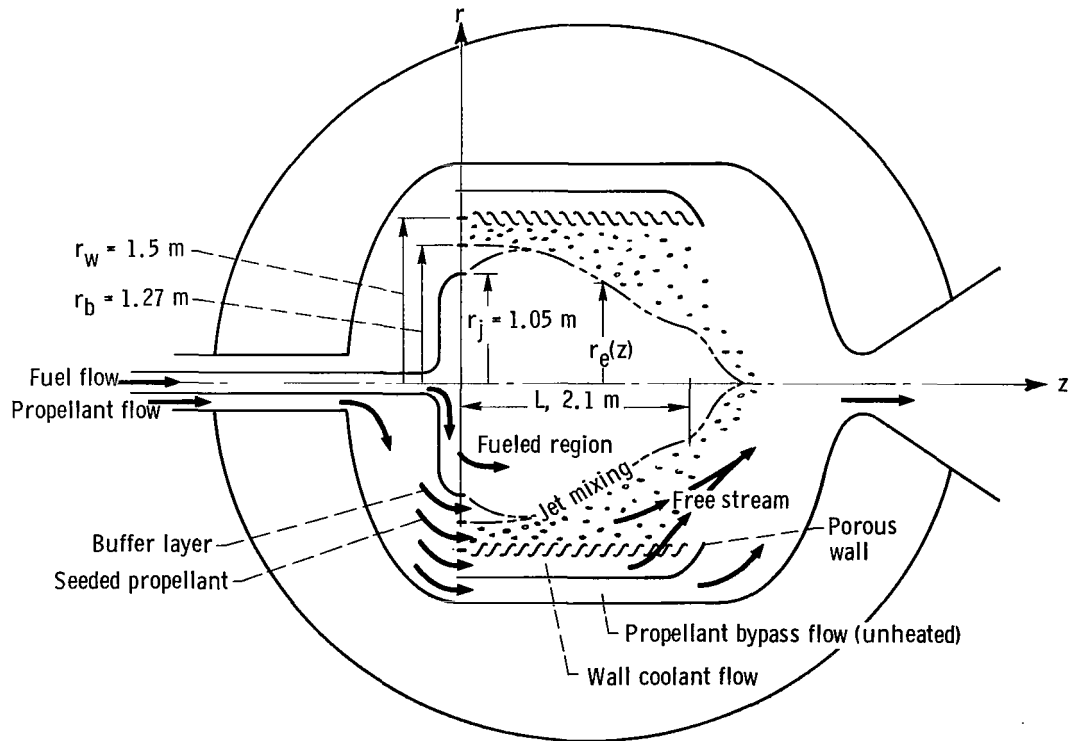
Past analyses have assumed radiation to be the dominant mode of heat transfer because of the high fuel and propellant temperatures. But reference 2 has shown that turbulent mixing is the dominant means of mass transfer in the fuel-propellant mixing process. Heat transfer by turbulent mixing could be important where temperature gradients or shear stresses, or both, are large. Three such regions exist in the coaxial-flow rocket. The first is near the inlet where large temperature gradients exist between the fuel and the propellant. A second is along the walls of the cavity and the nozzle, and a third is in the fuel-propellant jet mixing region. In the last two regions shear stresses would be large.

Three questions are to be answered in this report:

- (1) Does turbulent mixing transfer a significant fraction of the fission power from the fuel to the surrounding propellant?
- (2) Is the effect of turbulent mixing dependent on engine thrust or reactor pressure?
- (3) Is this estimate of the effect of turbulent mixing or heat transfer applicable to a wide range of operating conditions?



(a) Conceptual model.



(b) Representative cross section showing pertinent dimensions. (At $z = 0$, $r_e(0) = r_j$.)

Figure 1. - Coaxial-flow, gas-fueled nuclear rocket.

ROCKET OPERATING CONDITIONS

In order to perform the analysis, a suitable set of operating conditions must be selected. Reference 3 lists the following representative values for a first-generation gas-core nuclear rocket:

Specific impulse, I_{sp} , sec	1500
Fuel- to total-flow-rate ratio, η_f	1/31
Thrust, F , MN (Mlb)	0.445 to 4.45 (0.1 to 1.0)

From these values, the following mass flow rates may be calculated:

Exhaust, $\dot{m}_{ex} = F/(gI_{sp})$, kg/sec	34 to 340
Fuel, $\dot{m}_f = \eta_f \dot{m}_{ex}$, kg/sec	1.1 to 11.0
Propellant, $\dot{m}_p = (1 - \eta_f) \dot{m}_{ex}$, kg/sec	32.9 to 329

When a nozzle efficiency η_{noz} of 90 percent is assumed, the exhaust enthalpy is

$$h_{ex} = \frac{1}{2} \left(\frac{gI_{sp}}{\eta_{noz}} \right)^2 = 1.33 \times 10^8 \text{ J/kg} \quad (1)$$

Reference 4 studied the use of a buffer layer to reduce fuel-propellant mixing and concluded that mixing was minimized for $U_p/U_b = 5$ and approximately equal flow areas ($r_b = r_j + 1/2(r_w - r_j)$). For this study two-thirds of the propellant was bypassed, one-sixth of the propellant was used for wall cooling, and one-sixth of the propellant was injected coaxially to the fuel as the buffer layer and the seeded propellant.

Reference 3 also indicated that both the diameter and length of the reactor cavity should be approximately 3 meters. A cavity diameter of 3 meters and a cavity length of 2.1 meters were chosen for this analysis. The diameter of the fuel region at the inlet was assumed to be 2.1 meters. Therefore, the maximum fuel volume was 50 percent of the total cavity volume with the intermediate bypass mixing region neglected. References 5 to 7 indicate that the critical mass is between 10 and 100 kilograms.

When only radiation is considered, reference 8 found the average fuel temperature to be about 50 000 K. Therefore, the fuel is ionized about four times. According to the perfect gas law, the operating pressure is between 10^7 and 10^8 newtons per square meter (10^2 and 10^3 atm). (If not specified differently, the operating pressure was assumed to be 5.05×10^7 N/m² (500 atm).) The average propellant temperature can be calculated by assuming that all the heat is transferred from the fuel to the propellant between the fueled region and the porous wall. Because this propellant was assumed to be one-third of the total amount of propellant, the enthalpy at the exit of the cavity region

(prior to mixing with the bypassed coolant) must be three times the exhaust enthalpy. For a rocket with a specific impulse of 1500 seconds using hydrogen as the propellant, this exhaust enthalpy corresponds to a propellant temperature at the exit of the cavity region of about 10 000 K. The average propellant temperature in the cavity is about one-half this temperature, or 5000 K. When this temperature and the average fuel temperature are used, the average fuel density is three times the average propellant density.

The Reynolds number of the injected fuel is defined as

$$\text{Re}_j = \frac{\rho_j U_j r_j}{\mu_j} = \frac{\dot{m}_f}{\pi r_j U_j} \quad (2)$$

or, in terms of thrust,

$$\text{Re}_j = \frac{\eta_f F}{\pi r_j \mu_j} \quad (3)$$

For the range of thrusts considered, the Reynolds number for the fuel jet is between 7.67×10^3 and 7.67×10^4 .

The energy generated in the fuel and transferred directly to the propellant is between 3.97×10^3 and 3.97×10^4 megawatts where

$$Q_t = \dot{m}_p h_{ex} - Q_{mod} \quad (4)$$

The energy dissipated in the moderator Q_{mod} is taken to be 0.10 Q_t as given in reference 3.

The authors believe these operating conditions to be representative of first-generation gas-core nuclear rockets. Characteristics of such a rocket should be common to most gas-core nuclear rockets. Therefore, the conclusions drawn should be insensitive to the particular numerical choices made. A summary of the important operating conditions is given in table I.

ANALYSIS

The analysis is divided into three parts. The first section discusses the formulation of approximate laws for determining the properties of mixtures from the properties of their constituents. Second, a fluid dynamics analysis is used to determine the amount of turbulent mixing. Third, formulations of the heat-transfer equation are presented.

Mixture Properties

Approximate mixing laws must be known so that the properties of the fuel-propellant mixture may be calculated from known properties of the fuel and propellant. The properties needed for this analysis are the Rosseland mean absorption coefficient, the specific heat, the viscosity, and the fuel density.

The Rosseland mean absorption coefficient is based on the average thermal radiation cross section of a particle; thus, its mixing law is related to the atom fraction, or

$$a_R = a_{R,f}x + a_{R,p}(1 - x) \quad (5)$$

Since specific heat is defined on a mass basis, its mixing law is related to the mass fraction so that

$$C_p = C_{p,f}y + C_{p,p}(1 - y) \quad (6)$$

Viscosity is a transport property and therefore is not the linear sum of the viscosity of the constituents. Reference 9 gives the following mixing law for viscosity.

$$\mu = \frac{x\mu_f}{x + (1 - x)\varphi_{f,p}} + \frac{(1 - x)\mu_p}{x\varphi_{p,f} + (1 - x)} \quad (7)$$

where

$$\varphi_{f,p} = \frac{1}{\sqrt{8}} \left(1 + \frac{M_f}{M_p}\right)^{-1/2} \left[1 + \left(\frac{\mu_f}{\mu_p}\right)^{1/2} \left(\frac{M_p}{M_f}\right)^{1/4}\right]^2 \quad (8)$$

and

$$\varphi_{p,f} = \frac{1}{\sqrt{8}} \left(1 + \frac{M_p}{M_f}\right)^{-1/2} \left[1 + \left(\frac{\mu_p}{\mu_f}\right)^{1/2} \left(\frac{M_f}{M_p}\right)^{1/4}\right]^2 \quad (9)$$

By the perfect gas law, the fuel density is

$$\rho_f = \frac{M_f P_f}{RT} \quad (10)$$

and by the definition of the mole fraction, the fuel partial pressure is

$$P_f = xP_t \quad (11)$$

the mass and mole fractions and the average molecular weight are defined as follows:

$$y = \frac{\rho_f}{\rho_f + \rho_p} \quad (12)$$

$$x = \frac{P_f}{P_f + P_p} = \frac{y}{y + \left(\frac{M_f}{M_p}\right)(1 - y)} \quad (13)$$

$$\bar{M}_\alpha = \frac{\sum_i M_i n_{\alpha, i}}{\sum_i n_{\alpha, i}} \quad (14)$$

where $n_{\alpha, i}$ is the number density of the pure α substance of the i^{th} specie. These mixing laws are approximate, and they do not allow for a change in individual specie concentration when the individual substances are mixed. The authors assume these approximations to be sufficiently accurate for this analysis.

The Rosseland mean absorption coefficient for the propellant is given in reference 10. The data from which the specific heat and molecular weight were calculated are also given in this reference. The viscosity of the propellant was taken from references 11 and 12, and its molecular conductivity was obtained from reference 13.

The viscosity of the fuel from reference 11 was extrapolated to lower temperatures. The Rosseland mean absorption coefficient of the fuel is given in reference 14. The specific heat and molecular weight of the fuel were computed by the method given in reference 15 after modification to include charged particles. Fuel ionization potentials used in this calculation were provided by J. T. Waber, D. Lieberman, and D. T. Cromer of Los Alamos Scientific Laboratory. These potentials are presented in reference 8. References 16 and 17 describe related work.

Fluid Dynamics

In order to analyze the effect of turbulent mixing on heat transfer, the magnitude of the mixing must be determined from a fluid dynamics analysis. Reference 18 describes

a computer code for determining the isothermal, turbulent-jet mixing of two gases. This code was used to compute the axial mass flow rate \dot{m} , the eddy viscosity $\epsilon\rho$, and the containment factor I . Since the code considers only isothermal mixing, its results must be scaled by forming dimensionless groups which the authors assume will not be temperature dependent. This scaling process is only approximate since the energy equation was not solved by the code.

Two empirical eddy diffusivity correlations based on a characteristic length are used in the code. Before the fuel jet centerline velocity begins to change, a wake flow correlation is used in which the axial distance from the inlet is the characteristic length. Further downstream where the mixing is axisymmetric, a fully developed correlation is used. This correlation is based on the half radius, which is the point at which the velocity equals the average of the fuel centerline and propellant velocities.

The containment factor is defined as

$$I(z) = \frac{1}{\rho_j r_j^3} \int_0^z \int_0^{r_w} \rho y r' dr' dz' \quad (15)$$

where $I(z)$ is the amount of fuel contained in the cavity to axial position z .

The velocity ratios $U_p/U_j = 5$ and $U_p/U_j = 25$ and the density ratio $\rho_p/\rho_j = 3$, which were evaluated in the section ROCKET OPERATING CONDITIONS, were used as part of the code input. The mass fraction y , the dimensionless mass flow rate $\rho U/\rho_j U_j$, and the dimensionless turbulent viscosity $\epsilon\rho/r_j U_j \rho_j$ were taken from the code output. The dimensionless parameters y , $\rho U/\rho_j U_j$, and $(\epsilon\rho/\mu)/(r_j U_j \rho_j/\mu_j) = \epsilon^+/\text{Re}_j$ were assumed by the authors to be independent of temperature.

Heat Transfer

The relations governing radiant heat transfer in the coaxial-flow, gas-core nuclear rocket were developed in reference 8. This work must be extended to include turbulent mixing.

The analysis considers one-dimensional radial transfer of heat due to both thermal radiation and turbulent mixing. The formula

$$q = -K \frac{\partial T}{\partial r} \quad (16)$$

allows the definition of an effective thermal conductivity K where

$$K = K_{\text{rad}} + K_{\text{turb}} \quad (17)$$

The effective radiation conductivity K_{rad} is based on the Rosseland diffusion formulation of radiative transport. The effective turbulent conductivity K_{turb} is based on an empirically defined eddy diffusivity.

The effective radiation conductivity is inversely proportional to the Rosseland mean absorption coefficient and directly proportional to the temperature cubed. The resulting equation is

$$K_{\text{rad}} = \frac{16 \sigma T^3}{3 a_R} \quad (18)$$

The effective turbulent conductivity is equal to the eddy viscosity $\epsilon \rho$ times the specific heat so that

$$K_{\text{turb}} = \epsilon^+ \mu C_p \quad (19)$$

where

$$\epsilon^+ = \frac{\epsilon}{\nu}$$

$$\epsilon = \epsilon_h = \epsilon_m$$

The local heat-source strength is proportional to the local fuel density when the neutron flux is assumed to be uniform with respect to position and energy. When $\overline{Q}''' / \overline{\rho}_f$ is the coefficient of proportionality, the equation for local heat source strength is

$$Q''' = \overline{Q}''' \left(\frac{\rho_f}{\overline{\rho}_f} \right) \quad (20)$$

Performing a heat balance on the interior regions of the core results in a relation between the heat-source strength and the heat flux.

$$2\pi r q(r) = 2\pi \int_0^r r' Q'''(r') dr' \quad (21)$$

The average fuel density $\overline{\rho}_f$ is defined as the density of pure fuel at the system total pressure and at an average temperature defined implicitly by

$$2\pi \int_0^{r_e} \rho_f(\bar{T}, y) r' dr' \equiv 2\pi \int_0^{r_e} \rho_f(T, y) r' dr' \quad (22)$$

where y is the mass fraction at any radius and the fuel-propellant boundary r_e is the radius at which $y = 0.01$. The average fuel density is then $\bar{\rho}_f = \rho_f(\bar{T}, 1.0)$. The average power level \bar{Q}''' is related to heat flux at the fuel-propellant boundary and the average temperature. This relation can be found by combining equations (20) to (22)

$$\bar{Q}''' = \frac{r_e q_e \bar{\rho}_f}{\int_0^{r_e} \rho_f(\bar{T}, y) r' dr'} \quad (23)$$

The blackbody radiating temperature at the fuel-propellant boundary is defined by

$$q_e = \sigma T_e^{*4} \quad (24)$$

The actual temperature is some multiple of the boundary blackbody radiating temperature

$$T_e = \eta T_e^* \quad (25)$$

where $\eta = 1$ (based on ref. 8). The radial heat flux is given by

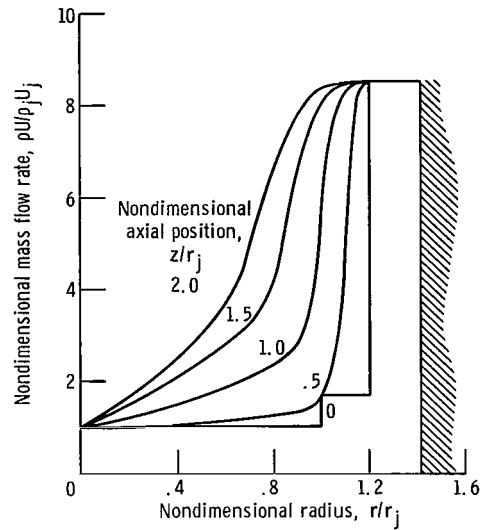
$$q_e = \frac{1}{2\pi r_e} \frac{Q_t}{r_j I(L)} \frac{dI}{d(z/r_j)} \quad (26)$$

Equations (16) to (25) are a set of equations which describe the heat-transfer process. Appendix A describes an iterative Runge-Kutta technique for solving these equations.

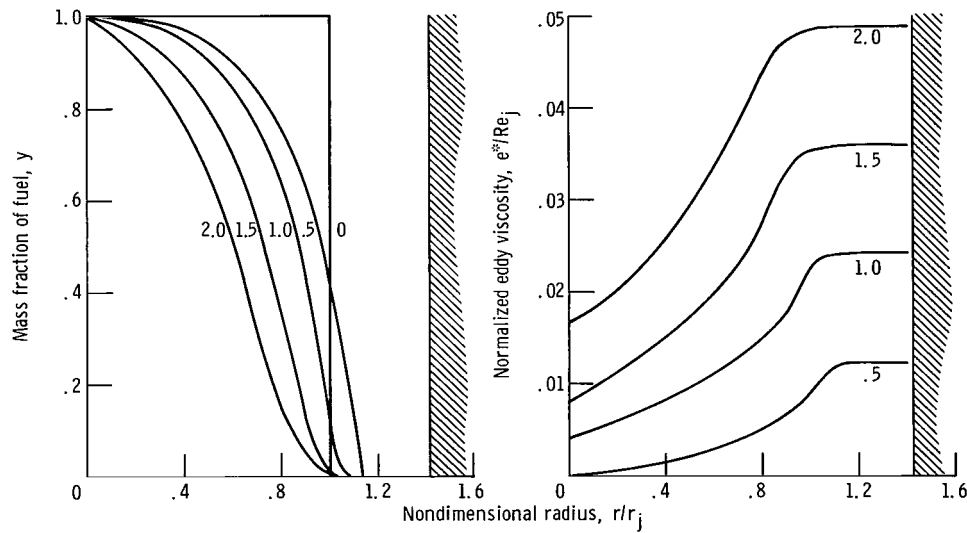
RESULTS AND DISCUSSION

The results obtained are discussed in this section. First, the gas mixing patterns and the eddy viscosities used are discussed. Next, the effective thermal conductivities due to both turbulence and thermal radiation are presented and compared. Finally, fuel temperatures in an engine are calculated first with turbulence neglected, and then with it included.

Figure 2(a) shows the dimensionless axial mass flow rate $\rho U / \rho_j U_j$ as a function of the dimensionless radius r/r_j for various values of the dimensionless length z/r_j . The



(a) Nondimensional mass flow rate. High-velocity outer stream first accelerates buffer layer then accelerates fueled region.



(b) Mass fraction of fuel. Fuel first diffuses into buffer layer then is eroded away by high-velocity propellant.

(c) Normalized eddy viscosity. Eddy viscosity at inlet is low and then increases with increasing axial position. Eddy viscosity is lower in fuel than in propellant.

Figure 2. - Nondimensional mass flow rate, mass fraction of fuel, and normalized eddy viscosity as functions of nondimensional radius for various axial positions.

fuel velocity was assumed to change instantly at the point $z = 0$, where the fuel enters the fuel region. At $z/r_j = 0.5$ the mass flow rate of the buffer layer is about one-half that of the free stream. The mass flow rate of the buffer layer approaches that of the free stream for $z/r_j = 1$, and, for $z/r_j > 1$, the fuel is accelerated by the free stream.

Figure 2(b) shows the fuel mass fraction as a function of r/r_j for various values of z/r_j . When a step change in the fuel mass fraction at $z = 0$ is assumed, the fuel radius is a maximum at $z/r_j = 0.5$. For $z/r_j > 1$ the slower moving buffer layer no longer exists. Therefore, the fuel diffuses into the high-velocity propellant and is swept away.

Figure 2(c) shows the normalized eddy viscosity ϵ^+/Re_j as a function of r/r_j for various z/r_j . At the inlet ϵ^+/Re_j is assumed to be zero. In general, ϵ^+/Re_j is almost constant in the propellant region and decays in the fuel region. The magnitude of ϵ^+/Re_j increases with increasing z/r_j .

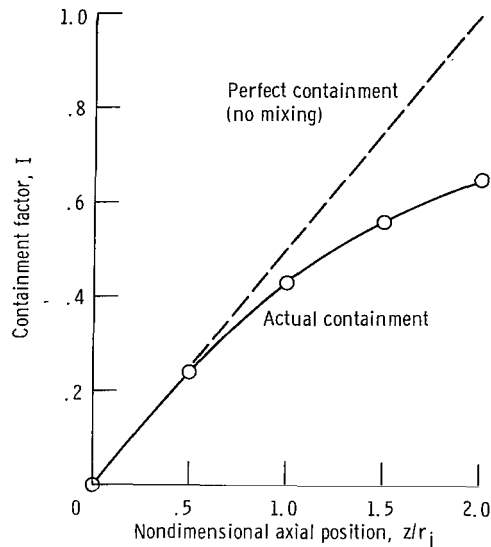


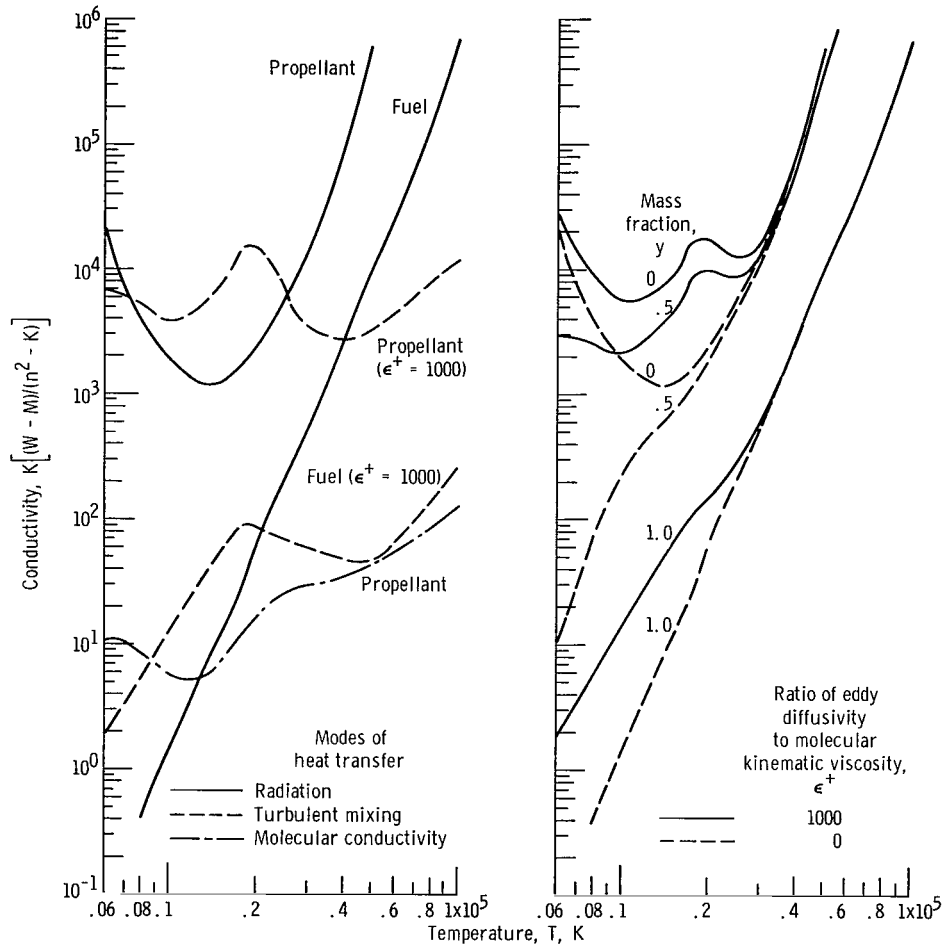
Figure 3. - Containment factor as function of nondimensional axial position. Near inlet there is very little mixing. Mixing process increases downstream, causing containment to fall below perfect containment line.

Figure 3 shows the containment factor I as a function of z/r_j . If there were perfect containment (no mixing), the slope of the line would be $1/2$. Since there is mixing, the actual line falls below the perfect containment line. The slope of this line is less than $1/2$ and decreases with increasing z/r_j . Physically, the mixing rate starts at low values and increases with increasing z/r_j .

Figures 2 and 3 show that the majority of the mixing occurs in the downstream half of the reactor. For a thrust of 2.5 meganewtons (0.5 Mlb), the Reynolds number for the

fuel jet is 38 300. For this Reynolds number, figure 2(c) shows that the dimensionless eddy viscosity ϵ^+ is between 200 and 2000 for $z/r_j \geq 1$. For the constant dimensionless eddy viscosity calculations, a value of 1000 was used.

Figure 4(a) shows the effective turbulent mixing and radiation conductivities for both the fuel and the propellant and the molecular conductivity for the propellant. The molecular conductivity of the fuel is expected to be one to two orders of magnitude less than that of the propellant because, although the electron densities are comparable, the specific heats differ by one or two orders of magnitude. The molecular conductivities are



(a) Conductivity for pure constituents for various modes of heat transfer. Propellant conductivities are several orders of magnitude higher than respective fuel conductivities. At high temperatures radiation conductivities are several orders of magnitude higher than turbulent conductivities.

(b) Combined conductivities for various mass fractions. Turbulence is important below temperatures of about 30 000 K. In general, mixtures of fuel and propellant tend to have conductivities similar to propellant.

Figure 4. - Conductivity as function of temperature at pressure of 5.05×10^7 newtons per square meter (500 atm).

composed mainly of an electron conductivity and a reaction conductivity which is proportional to the specific heat. In this temperature range, the reaction conductivity is dominant. The effective radiation and turbulent mixing conductivities for the propellant are also one to two orders of magnitude higher than the corresponding fuel conductivities. Radiation is the dominant mode of heat transfer for temperatures greater than 25 000 K, and for temperatures greater than 50 000 K radiation is several orders of magnitude greater than turbulent mixing. Below 20 000 K turbulent mixing is the dominant mode of heat transfer. In the range of temperatures shown, molecular conduction is negligible.

By using the mixing laws given in the section ANALYSIS, the total effective conductivities were calculated as a function of temperature for various mass fractions. These effective conductivities are shown in figure 4(b) with and without turbulent mixing. At temperatures below 30 000 K turbulent mixing greatly increases the total effective conductivity, while above 30 000 K the effect is small. Figures 4(a) and (b) also show that the heat-transfer process is a variable-properties problem, so that the total conductivity is a strong function of the propellant properties.

For the operating condition given herein, an average radial temperature gradient of 42 500 K per meter was calculated. When a reactor power of 20 000 megawatts (2.5-MN thrust) and the heat-transfer area of a cylinder whose radius and length are 2.1 meters are used, an average heat flux of 1.42×10^3 megawatts per square meter was calculated. The average total conductivity must therefore be about 33 kilowatts per meter per Kelvin. This conductivity corresponds to a fuel temperature of about 63 000 K or a propellant temperature of 35 000 K. Figure 4(b) shows that at these temperatures turbulent mixing has a negligible effect on the total conductivity. Figure 4(a) shows that for turbulent mixing to be dominant at these temperatures, the estimate of the eddy viscosity must be in error by several orders of magnitude.

Figures 5(a) and (b) show the effect of turbulent mixing on the radial temperature profiles at various axial locations for a rocket operating at a pressure of 5.05×10^7 newtons per square meter (500 atm), a specific impulse of 1500 seconds, and thrusts of 0.445 and 4.45 Meganewtons (0.1 and 1.0 Mlb), respectively. Turbulent mixing reduces the temperature in the downstream jet mixing region by about 30 percent for a thrust of 0.445 Meganewton (0.1 Mlb). At a thrust of 4.45 Meganewtons (1.0 Mlb) the change in temperature was about 90 percent. The effect near the inlet or centerline is less than 1 percent. Comparison of figures 5(a) and (b) shows that at higher thrusts the turbulent mixing effect is greater. Turbulent mixing reduces temperatures the most in regions where the fuel mass fraction is lowest. Therefore, the effect of turbulent mixing on the average fuel temperature is less than 1 percent.

Figure 6 shows the effect of turbulent mixing on the average fuel temperature as a function of thrust for various pressures. Turbulent mixing affects the average fuel temperature by less than 1 percent for thrusts from 0.445 to 4.45 Meganewtons (0.1 to

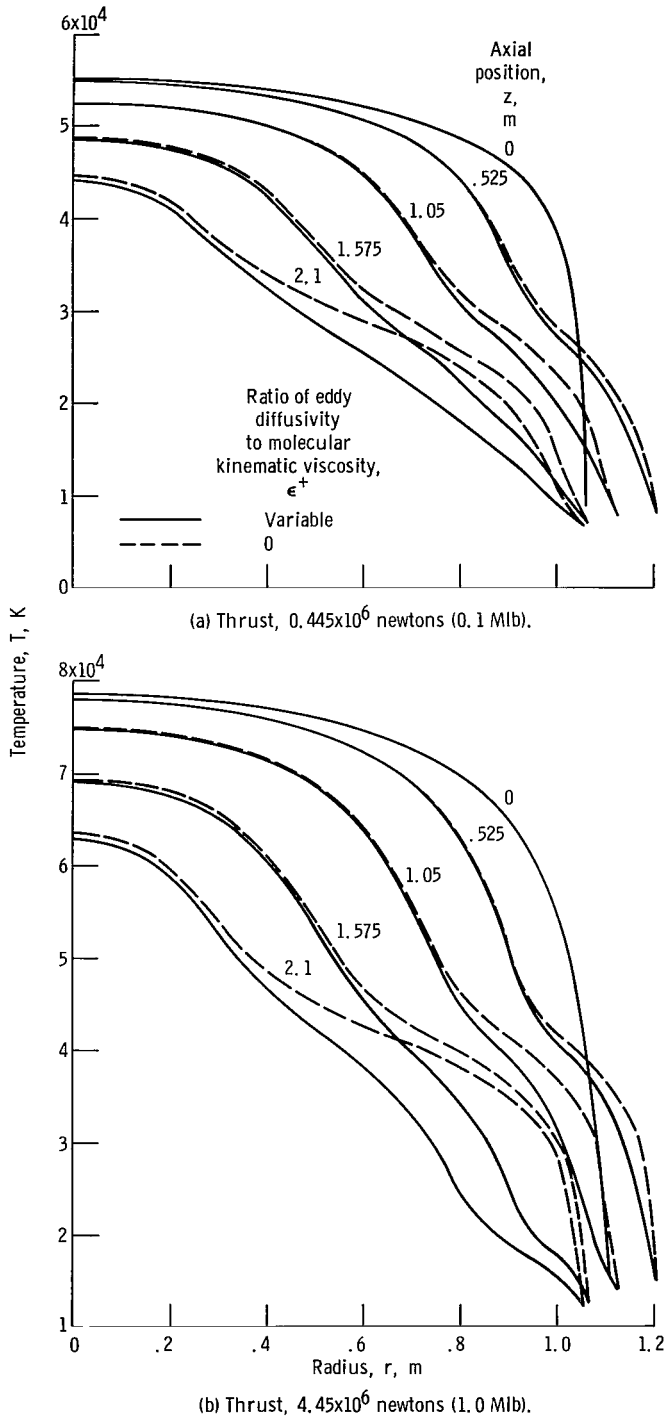


Figure 5. - Radial temperature profiles at various axial positions for specific impulse of 1500 seconds and pressure of 5.05×10^7 newtons per square meter (500 atm). Turbulence reduces temperature in downstream annular region. Temperatures near inlet and centerline are not very sensitive to turbulent effects.

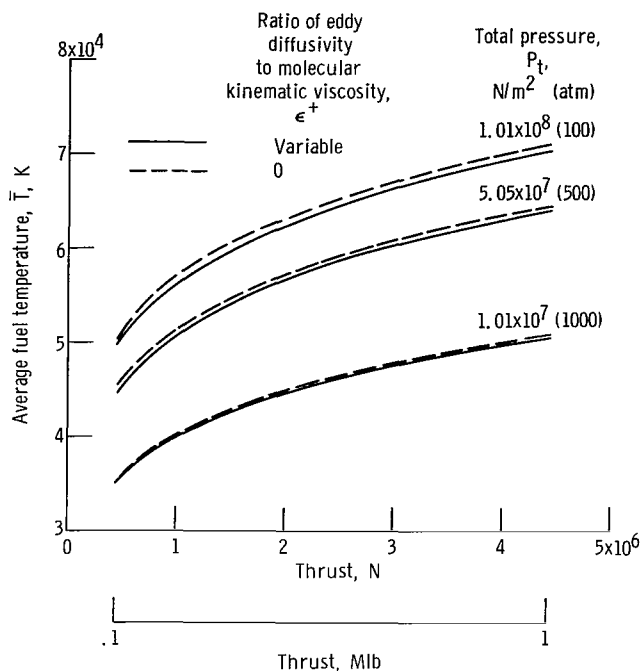


Figure 6. - Average fuel temperature as function of thrust for various pressure levels. Turbulence has very little effect on average fuel temperatures. Turbulence effect increases slightly with increasing pressure and is almost independent of thrust.

1.0 Mlb) and for pressures from 10.1 to 101.0 meganewtons per square meter (100 to 1000 atm). The magnitude of the effect seems to be independent of thrust but slightly dependent on pressure. The authors conclude that in the range of conditions considered, heat transfer by turbulent mixing can be neglected in estimating the average fuel temperature.

The average fuel temperatures in this report are about 15 percent higher than those given in reference 8. That reference considered a fueled region with a larger length-to-diameter ratio; temperatures were calculated only at the midplane of the fueled region. The axially averaged fuel temperatures in this report correspond more closely to the step fuel distribution, rather than the Gaussian fuel distribution of reference 8. This correspondence is partly due to the fact that the consideration in this report of buffer layer, wall coolant, and bypass flow resulted in reduced mixing.

CONCLUSIONS

From this study of heat transfer in a coaxial-flow, gas-fueled nuclear rocket with a specific impulse of 1500 seconds and a thrust between 0.445 and 4.45 meganewtons (0.1 and 1.0 Mlb) at an operating pressure of 5.05×10^7 newtons per square meter (500 atm)

and for a dimensionless turbulent viscosity ϵ^+ of 1000, the following conclusions were drawn:

1. Radiation is the dominant mode of heat transfer for temperatures above 25 000 K, and turbulent mixing is the dominant mode below 20 000 K.
2. For temperatures greater than 50 000 K, effective radiation conductivities are several orders of magnitude greater than effective turbulent conductivities.
3. The heat-transfer process is not a constant-properties problem. For typical reactor heat fluxes and temperature gradients the necessary effective conductivity corresponds to fuel temperatures of about 63 000 K and propellant temperatures of about 35 000 K.
4. The effective conductivity of a mixture of fuel and propellant is a strong function of the properties of the pure propellant and a lesser function of the properties of the pure fuel.

For variable eddy viscosity, a function of both radial and axial position, the effects of turbulent mixing on the local and average temperatures are as follows:

5. Near the inlet and the centerline of the reactor, the local temperature is reduced by less than 1 percent when turbulent mixing is included.
6. The maximum change in local temperature at a thrust of 0.445 meganewton (0.1 Mlb) was approximately 30 percent, while at 10 times this thrust (4.45 MN (1.0 Mlb)) the change was equal to about 90 percent.
7. The change in average fuel temperature is about 1 percent for all thrust levels.
8. The change in average fuel temperatures is not very sensitive to pressure levels. It ranges from about 1/4 percent at 1.07×10^7 newtons per square meter (100 atm), while at 10 times this pressure it was about 1 percent.

The preceding conclusions were drawn for a particular reactor geometry and flow distribution. Although these choices could affect eddy viscosities, the changes would not be by orders of magnitude.

Lewis Research Center,
National Aeronautics and Space Administration,
Cleveland, Ohio, August 6, 1968,
122-28-02-33-22.

APPENDIX A

NUMERICAL ANALYSIS

This appendix describes the numerical methods used to solve the equations derived in the heat-transfer analysis section. These equations are the energy equation and the equations defining average temperature, average density, average source strength, and the variation of the source strength. In these equations the fuel-propellant boundary temperature and heat flux are known boundary conditions.

The energy equation is a nonlinear integral equation and must be solved by an iterative process. In the iterative process a temperature distribution was assumed. Based on this assumption the average quantities of temperature, density, and source strength were calculated. From these average quantities a new temperature distribution was calculated. This process was repeated until the average quantities changed by less than 0.01 percent.

The initial temperature-distribution calculation was based on an initially uniform source-strength distribution. For this source-strength distribution ($\rho_f/\bar{\rho}_f \equiv 1$), the average source strength is

$$\bar{Q}''' = \frac{2q_e}{r_e} \quad (A1)$$

For this average source strength the heat flux is

$$q = \frac{\bar{Q}'''r}{2} \quad (A2)$$

When the heat flux and Fourier's conduction law are known, a Runge-Kutta method can be used to calculate an initial guess for temperature distribution from the outer edge inward to the center line. If a uniform grid is set up in the radial direction r with Δr being the grid spacing, an approximate relation can be set up between adjacent grid points:

$$q_n = \frac{-K_n(T_{n+1} - T_n)}{\Delta r} \quad (A3)$$

Equation (A3) can be solved by using a modified Newton-Raphson technique. For numerical purposes equation (A3) was rewritten in the following forms:

$$0 = \ln \left[\frac{-K_n(T_{n+1} - T_n)}{\Delta r q_n} \right] \quad (A4)$$

$$W = \ln \left(\frac{T_n - T_{n+1}}{T_{n+1}} \right) \quad (\text{A5})$$

Equations (A4) and (A5) were used because of large property variations. For this temperature distribution the average temperature was calculated by using the following definition:

$$\int_0^r e^{\rho_f(\bar{T}, y)} r \, dr \equiv \int_0^r e^{\rho_f(T, y)} r \, dr \quad (\text{A6})$$

In order to calculate the average temperature, the Newton-Raphson technique was again used.

For this average temperature the average density was calculated as

$$\bar{\rho}_f \equiv \rho_f(\bar{T}, 1) \quad (\text{A7})$$

With this average density the average source strength was calculated as

$$\bar{Q} = \frac{r e^q \bar{\rho}_f}{\int_0^r e^{\rho_f(\bar{T}, y)} r \, dr} \quad (\text{A8})$$

With the calculated distribution and the calculated average quantities used as an initial guess, a Newton-Raphson technique was used to solve for the correct value of the average source strength. The following equation was used in the Newton-Raphson technique

$$f(\bar{Q}'') = \bar{Q}'' - \bar{Q}''_{\text{guess}} \quad (\text{A9})$$

where \bar{Q}''_{guess} is the \bar{Q}''_{cal} from the previous iteration and \bar{Q}''_{cal} is calculated by using equation (A10) instead of (A2).

$$q(r) = \frac{\bar{Q}''}{r} \int_0^r \left(\frac{\rho_f}{\bar{\rho}_f} \right)_{r'} \, d'r' \quad (\text{A10})$$

This process is repeated using equations (A10) and (A4) to (A8) until a convergence criterion is met. The convergence criterion used in all the modified Newton-Raphson techniques was based on the absolute value of the relative change in the independent variable being less than some specified quantity.

The mass fraction was obtained from reference 18 by using a linear interpolation method. The mass fraction is a function of the radial position r . The value for eddy diffusivity is also obtained from reference 18 in the same manner.

The properties used to calculate conductivity and the density of the fuel are computed from tables. The properties for both fuel and propellant are viscosity, specific heat, Rosseland mean absorption coefficient, and molecular weight. These properties are a function of temperature and were computed by log-log interpolation.

APPENDIX B

SYMBOLS

a_R	Rosseland mean absorption coefficient, 1/m	Δr	increment in radial position, m
c_p	specific heat, J/(kg)(K)	r_e	fuel-propellant boundary, $y = 0.01$
F	thrust, N	T	temperature, K
g	gravitational acceleration, 9.8 m/sec^2	U	axial velocity, m/sec
h	enthalpy, J/kg	W	function defined in eq. (A5)
I	containment factor, defined in eq. (15)	x	mole fraction of fuel
I_{sp}	specific impulse (thrust divided by weight flow rate where acceleration of gravity is 9.8 m/sec^2), sec	y	mass fraction of fuel
K	conductivity, J-m/(m ²)(sec)(K)	z	axial position, m
L	length, m	ϵ	eddy diffusivity of momentum, m ² /sec
M	molecular weight	ϵ^+	ratio of eddy diffusivity to molecular kinematic viscosity
\dot{m}	mass flow rate, kg/sec	η	ratio of actual temperature to blackbody temperature at fuel-propellant boundary
n	particle density, 1/m ³	η_f	ratio of fuel flow rate to total flow rate
P	pressure, N/m ²	η_{noz}	ratio of actual I_{sp} to ideal I_{sp} for a nozzle
Q	power, J/sec	μ	viscosity, (N)(sec)/m ²
Q'''	volumetric heat generation, J/(m ³)(sec)	ν	kinematic viscosity, m ² /sec
q	heat flux, J/(m ²)(sec)	ρ	mass density, kg/m ³
R	gas constant, 8.3143 J/(K)(mole)	σ	Stefan-Boltzmann constant, $5.67 \times 10^{-8} \text{ W/(m}^2\text{)(K}^4\text{)}$
Re	Reynolds number	φ	function defined in eqs. (8) and (9)
r	radius, m		
r'	radial dummy variable of integration		

Subscripts:

b	buffer layer	n	dummy index referring to radial position
cal	calculated on present iteration	p	propellant
e	edge of fuel	rad	radiation
ex	exhaust	t	total
f	fuel	turb	turbulence
guess	guess of calculation on present iteration	w	cavity wall
h	heat	α	dummy index referring to fuel or propellant
j	jet, fuel stream at inlet conditions	Superscripts:	
i	dummy index referring to species summed over	—	average
m	momentum	*	blackbody conditions
mod	moderator		

REFERENCES

1. McLafferty, G. H. ; Michels, H. H. ; Lathem, T. S. ; and Roback, R. : Analytical Study of Hydrogen Turbopump Cycles for Advanced Nuclear Rockets. Rep. D-910093-19, United Aircraft Corp. (NASA CR-68988), Sept. 1965, App. 1.
2. Ragsdale, Robert G. ; Weinstein, Herbert; and Lanzo, Chester D. : Correlation of a Turbulent Air-Bromine Coaxial-Flow Experiment. NASA TN D-2121, 1964.
3. Rom, Frank E. ; and Ragsdale, Robert G. : Advanced Concepts for Nuclear Rocket Propulsion. NASA SP-20, 1962, pp. 3-15.
4. Ragsdale, Robert G. : Effects of a Momentum Buffer Region on the Coaxial Flow of Dissimilar Gases. NASA TN D-3138, 1965.
5. Pincock, G. D. ; and Kunze, J. F. : Cavity Reactor Critical Experiment. Vol. 1. General Electric Co. (NASA CR-72234), Sept. 6, 1967.
6. Miraldi, Floro; Nelson, George W. ; Holmberg, Gary; and Skoff, Gerald: Neutron Flux Distributions: (Experiment vs. Theory) For a Water Reflected-Spherical Cavity System. Case Inst. Tech. (NASA CR-72231), Dec. 31, 1966.
7. Hyland, Robert E. ; Ragsdale, Robert G. ; and Gunn, Eugene F. : Two-Dimensional Criticality Calculations of Gaseous-Core Cylindrical-Cavity Reactors. NASA TN D-1575, 1963.
8. Kascak, Albert F. : Estimates of Local and Average Fuel Temperatures in a Gaseous Nuclear Rocket Engine. NASA TN D-4164, 1967.
9. Bird, R. Byron; Stewart, Warren E. ; and Lightfoot, Edwin N. : Transport Phenomena. John Wiley & Sons, Inc., 1960, p. 24.
10. Krascella, N. L. : Tables of the Composition, Opacity, and Thermodynamic Properties of Hydrogen at High Temperatures. NASA SP-3005, 1963.
11. Schneiderman, S. B. : Theoretical Viscosities and Diffusivities in High-Temperature Mixtures of Hydrogen and Uranium. NASA CR-213, 1965.
12. Svehla, Roger A. : Thermodynamic and Transport Properties for the Hydrogen-Oxygen System. NASA SP-3011, 1964.
13. Grier, Norman T. : Calculation of Transport Properties of Ionizing Atomic Hydrogen. NASA TN D-3186, 1966.
14. Krascella, N. L. : Theoretical Investigation of the Opacity of Heavy-Atom Gases. Rep. D-910092-4, United Aircraft Corp. (NASA CR-69001), Sept. 1965.

15. Zeleznik, Frank J.; and Gordon, Sanford: A General IBM 704 or 7090 Computer Program for Computation of Chemical Equilibrium Compositions, Rocket Performance, and Chapman-Jouguet Detonations. NASA TN D-1454, 1962.
16. Liberman, D.; Waber, J. T.; and Cromer, Don T.: Self-Consistent-Field Dirac-Slater Wave Functions for Atoms and Ions. I. Comparison with Previous Calculations. Phys. Rev., vol. 137, no. 1A, Jan. 4, 1965, pp. 27-34.
17. Cowan, R. D.; Larson, A. C.; Liberman, D.; Mann, J. B.; and Waber, J.: Statistical Approximation for Exchange in Self-Consistent-Field Calculations of the Ground State of Neutral Argon. Phys. Rev., vol. 144, no. 1, Apr., 1966, pp. 5-7.
18. Donovan, Leo F.; and Todd, Carroll A.: Computer Program for Calculating Isothermal, Turbulent Jet Mixing of Two Gases. NASA TN D-4378, 1968.

TABLE I. - OPERATING CONDITIONS

Parameter	Range	Value used
Total reactor power, MW	3970 to 39 700	19 850
Specific impulse, I_{sp} , sec	-----	1500
Thrust, F, MN	0. 445 to 4. 45	2. 22
Fuel- to total-flow-rate ratio, η_f	-----	1/31
Total mass flow rate, \dot{m}_{ex} , kg/sec	34 to 340	170
Fuel mass flow rate, \dot{m}_f , kg/sec	1. 1 to 11. 0	5. 5
Propellant mass flow rate, \dot{m}_p , kg/sec	32. 9 to 329	164
Pressure, P, MN/m ²	10. 1 to 101	50. 5
Nozzle efficiency, η_{noz}	-----	0. 90
Propellant inlet temperature, K	-----	1600
Exhaust enthalpy, h_{ex} , MJ/kg	-----	133
Ratio of propellant to buffer layer velocity, U_p/U_b	-----	5
Ratio of propellant bypassed to total propellant flow	-----	2/3
Ratio of propellant used for wall cooling to total propellant flow	-----	1/6
Ratio of injected propellant velocity to fuel velocity	-----	25
Cavity diameter, m	-----	3
Cavity length, m	-----	2. 1
Inlet of fuel region, m	-----	2. 1
Inlet of buffer layer, m	-----	2. 55
Total heat dissipated in moderator, percent	-----	10

FIRST CLASS MAIL

POSTMASTER: If Undeliverable (Section 158
Postal Manual) Do Not Return

"The aeronautical and space activities of the United States shall be conducted so as to contribute . . . to the expansion of human knowledge of phenomena in the atmosphere and space. The Administration shall provide for the widest practicable and appropriate dissemination of information concerning its activities and the results thereof."

— NATIONAL AERONAUTICS AND SPACE ACT OF 1958

NASA SCIENTIFIC AND TECHNICAL PUBLICATIONS

TECHNICAL REPORTS: Scientific and technical information considered important, complete, and a lasting contribution to existing knowledge.

TECHNICAL NOTES: Information less broad in scope but nevertheless of importance as a contribution to existing knowledge.

TECHNICAL MEMORANDUMS: Information receiving limited distribution because of preliminary data, security classification, or other reasons.

CONTRACTOR REPORTS: Scientific and technical information generated under a NASA contract or grant and considered an important contribution to existing knowledge.

TECHNICAL TRANSLATIONS: Information published in a foreign language considered to merit NASA distribution in English.

SPECIAL PUBLICATIONS: Information derived from or of value to NASA activities. Publications include conference proceedings, monographs, data compilations, handbooks, sourcebooks, and special bibliographies.

TECHNOLOGY UTILIZATION PUBLICATIONS: Information on technology used by NASA that may be of particular interest in commercial and other non-aerospace applications. Publications include Tech Briefs, Technology Utilization Reports and Notes, and Technology Surveys.

Details on the availability of these publications may be obtained from:

SCIENTIFIC AND TECHNICAL INFORMATION DIVISION
NATIONAL AERONAUTICS AND SPACE ADMINISTRATION
Washington, D.C. 20546